NUCLEAR SCIENCE AND TECHNIQUES **25**, 050501 (2014)

A method of estimating and subtracting the hydrogen background in the natural carbon target used in the ^{12}C + ^{12}C experiment*

QU Wei-Wei (屈卫卫),[1,2] ZHANG Gao-Long (张高龙),[1,2,†] Satoru Terashima,[1,2] Isao Tanihata,[1,2,3] GUO Chen-Lei (郭晨雷),[1,2] and LE Xiao-Yun (乐小云)[1,2]

[1]*School of Physics and Nuclear Energy Engineering, Beihang University, Beijing 100191, China*
[2]*International Research Center for Nuclei and Particles in the Cosmos, Beihang University, Beijing 100191, China*
[3]*Research Center for Nuclear Physics, Osaka University, Osaka 567-0047, Japan*

(Received March 3, 2014; accepted in revised form May 1, 2014; published online September 23, 2014)

The experimental data of $100A$ MeV $^{12}\mathrm{C} + {}^{12}\mathrm{C}$ elastic scattering are checked by using two-body kinematic calculation and $^{12}\mathrm{C} + \mathrm{p}$ elastic scattering. It is shown that the measured data are true and reliable. In the paper, the transformation between the excited energy spectra of the $^{12}\mathrm{C} + {}^{12}\mathrm{C}$ system and the ground state energy spectra of the $^{12}\mathrm{C} + \mathrm{p}$ system is introduced. The method of subtraction of the hydrogen background in the natural carbon target used in the experiment is elaborately described and the results are discussed. It is indicated that this method of subtraction of hydrogen background is reasonable and can be used in the data analysis. Based on the elastic scattering cross section of the previous experiment of $^{12}\mathrm{C}+\mathrm{p}$ at $95.3A$ MeV, the hydrogen content entered into the reaction is analyzed. The final hydrogen content in the natural carbon target is $(2.73 \pm 0.12)\%$.

Keywords: Elastic scattering, Subtraction background, Hydrogen content

DOI: 10.13538/j.1001-8042/nst.25.050501

I. INTRODUCTION

The role of the three-body-force (TBF) in complex nuclear systems is one of the key issues not only in nuclear physics but also in nuclear astrophysics relevant to high-density nuclear matter, such as neutron stars and supernova explosions. In nuclear collisions, elastic scattering can provide important information on the nucleon-nucleon (NN) and nucleus-nucleus (AA) interaction. Recently in Ref. [1–7] a double folding model (DFM) with a new type of complex G-matrix interaction including the TBF, was developed. They applied it to calculate the optical potential of $100A$–$400A$ MeV $^{12}\mathrm{C} + {}^{12}\mathrm{C}$ elastic scattering. It was indicated that the real part of the optical potential changes its character from attraction to repulsion as the incident energy increases. The angular distribution of $^{12}\mathrm{C} + {}^{12}\mathrm{C}$ elastic scattering shows a different diffraction transition with and without the TBF effect. Through this evolution of optical potential and angular distribution of elastic scattering with an increase of incident energies, the contributions of TBF and tensor force can be extracted [5]. However, so far there are not many theoretical and experimental studies for heavy ions at higher energies than those of deuteron [8]. Therefore, the angular distribution of $^{12}\mathrm{C}$ on $^{12}\mathrm{C}$ elastic scattering needs to be experimentally measured in the incident energy range of $100A$–$400A$ MeV. Through the precise measurement of elastic scattering, the repulsive nature of optical potential can be explained and the transition energy from attraction to repulsion of the real part in optical potential can be determined. It can provide important information about the TBF effect, the medium effect of high density nuclear matter, the energy dependence of TBF, and the role of tensor force.

II. EXPERIMENTAL SECTION

Firstly, the $100A$ MeV $^{12}\mathrm{C} + {}^{12}\mathrm{C}$ experiment was performed in Research Center for Nuclear Physics (RCNP) at Osaka University. The angular distribution was precisely obtained using the magnetic spectrometer, "Grand Raiden". This magnetic spectrometer has excellent ion-optical properties [9]. In order to make full use of the magnetic spectrometer, the beam was transported under the achromatic focusing along the WS beamline [10]. During the experiment we used a $1.181\,\mathrm{mg/cm^2}$-thickness natural carbon target and a $11.40\,\mathrm{mg/cm^2}$-thickness $(\mathrm{CH_2})_\mathrm{n}$ target. The TOF-ΔE signals, which were obtained from focal plane detectors, were used for particle identification. The details of focal plane detectors are described in Ref. [11]. After particle identification, the two dimensional plots of outgoing $^{12}\mathrm{C}$ particle excitation energies with laboratory angles were obtained when the central angle of the magnetic spectrometer was set to 2.0°, as shown in Fig. 1. We can clearly observe three horizontal bands which correspond to the ground state, $4.44\,\mathrm{MeV}$ (2^+) and $9.65\,\mathrm{MeV}$ (3^-) excited state of $^{12}\mathrm{C} + {}^{12}\mathrm{C}$ scattering. However, another tilted band crossing with the horizontal bands exists in Fig. 1. It increases the number of $^{12}\mathrm{C} + {}^{12}\mathrm{C}$ scattering events, especially at small angles. The contribution of this part cannot be neglected. In comparison with those from the excited states of $^{12}\mathrm{C}$ on $^{12}\mathrm{C}$ scattering, it is much larger at the smaller angles. So if the contribution of the tilted band is not subtracted, the differential cross section of $^{12}\mathrm{C}$ on $^{12}\mathrm{C}$ scattering can be affected. In the paper, we introduce a method to subtract this disturbance and obtain the content on the experimental target.

* Supported by the Innovation Foundation of BUAA for PhD Graduates and National Natural Science Foundation of China (Nos. 11035007, 11235002 and 11175011)
† Corresponding author, zgl@buaa.edu.cn

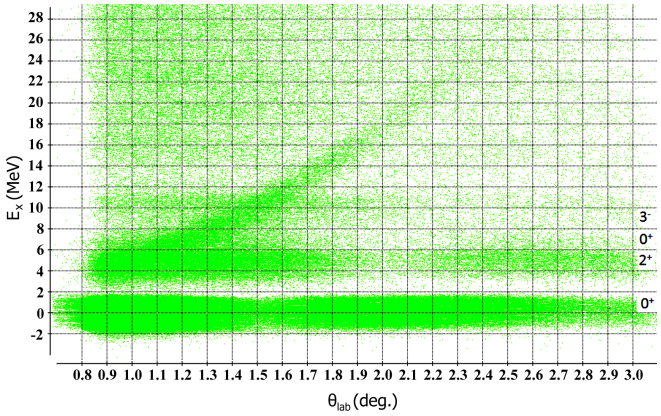

Fig. 1. (Color online) The two dimensional plot of outgoing ^{12}C particles excitation energies with laboratory angles when the central angle of the magnetic spectrometer was set to 2.0° for 100A MeV ^{12}C + ^{12}C scattering.

III. RESULTS AND DISCUSSION

Firstly, we compared the results of Fig. 1 on the natural target with that on the $(CH_2)_n$ target. The results are similar. Moreover, there was no tilted band in other plots on the natural carbon target at larger angles. So it is concluded that the tilted band is from ^{12}C on hydrogen scattering. Second, we checked the experimental data on the basis of the relativistic kinematics calculation. For reaction $A(a,b)B$, a, A, b, and B represent the projectile, the target nucleus, the scattered particle, and the recoiled nucleus, respectively. According to the definition of Q (reaction energy),

$$Q = K_B + K_b - K_a - K_A, \tag{1}$$

where K_a, K_A, K_b, and K_B denote the kinetic energies of the projectile, the target, the scattered particles, and the recoiled particles, respectively. Here, $K_A = 0$. According to the momentum conservation

$$p_B^2 = p_a^2 + p_b^2 - 2p_a p_b \cos\theta, \tag{2}$$

where p_a, p_b, and p_B, respectively represent the momentum of the projectile, the scattered nucleus, and the recoiled nucleus. θ is the scattering angle in the laboratory frame. If the relativistic is considered, the relationship between momentum and kinetic energy can be obtained

$$p_i = \sqrt{K_i^2 + 2K_i m_i}, \tag{3}$$

where m_i denotes the rest mass of nuclei. $i = a, A, b$, and B represent the projectile, the target nucleus, the scattered nucleus, and the recoiled nucleus, respectively. From Eqs. (1), (2), and (3), it can be obtained

$$Q = K_b - K_a - m_B + \sqrt{m_B^2 + \Delta}, \tag{4}$$

where

$$\Delta = K_a^2 + 2K_a m_a + K_b^2 + 2K_b m_b - 2\sqrt{(K_a^2 + 2K_a m_a)(K_b^2 + 2K_b m_b)}\cos\theta. \tag{5}$$

Through Eq. (4), for the ground state of ^{12}C + p and the excited states of ^{12}C + ^{12}C at 100A MeV incident energy, it is shown that the first excited state 4.4 MeV (2_1^+) of ^{12}C + ^{12}C scattering and the ground state of ^{12}C + p cross at 1.015°. The 9.64 MeV (3_1^-) state of ^{12}C + ^{12}C and the ground state of ^{12}C + p cross at 1.5°. The influence of the beam uncertainty (including the beam angular and beam size shift, which is about 2%) can be neglected for the calculation of cross angles. From Fig. 1, we can clearly see that the crossing angles are about 1.0° and 1.5°, which are consistent with the calculation. It proves the authenticity of the experimental data.

A. Subtraction of hydrogen disturbance in target

For easy selection of ^{12}C + p events, we convert the energy spectrum of ^{12}C + ^{12}C, shown in Fig. 1 to that of ^{12}C + p system, which is shown in Fig. 2.

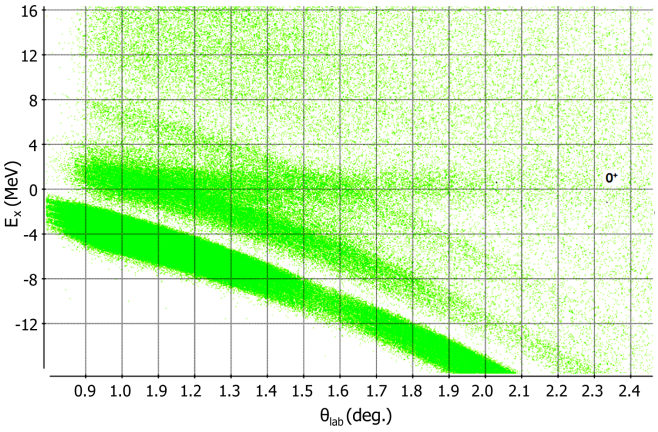

Fig. 2. (Color online) The two dimensional plot of outgoing ^{12}C particle excitation energies with laboratory angles of ^{12}C + p elastic scattering at 100A MeV.

During the conversion we used a polynomial function to rotate it. The rotation has to obey the rules. The excitation energy cannot change with the angles and the excitation energy of the ground state must stay zero. Finally we get the Eq. (6):

$$Q' = 0.0275\theta^4 + 0.0333\theta^3 + 2.9658\theta^2 + 3.4918\theta - 2.2786 + Q, \tag{6}$$

where Q' and Q represent the outgoing ^{12}C excitation energies of the ^{12}C + p and ^{12}C + ^{12}C systems, respectively. The uncrossed region of 1.7°–2.2° is selected, as it is mainly caused by ^{12}C + p elastic scattering. Fig. 3 shows the outgoing ^{12}C excitation energy spectrum at 1.8° and the fitting results. This method was applied to the other angles, we can obtain the real number of reactions with hydrogen and the width σ of the Gaussian distribution.

The differential cross sections of 96 MeV p + ^{12}C elastic scattering in Ref. [12] in the center of mass frame was converted to that of ^{12}C + p elastic scattering in the laboratory frame with the incident energy 95.3A MeV as shown in

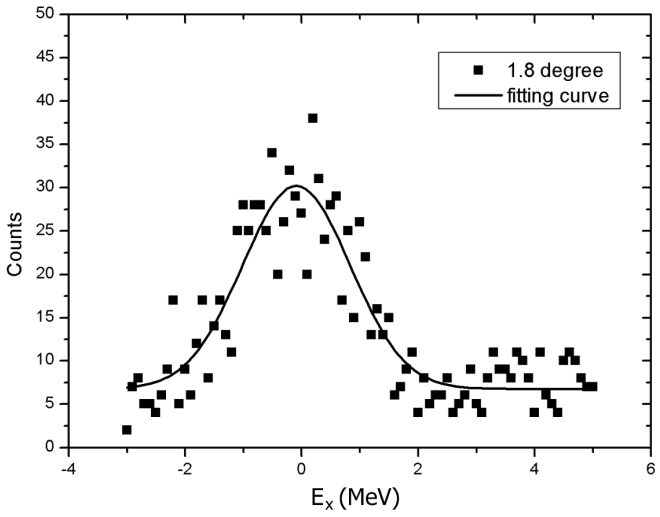

Fig. 3. The selection of the excitation energy spectrum at 1.8° in the uncrossed region of Fig. 2 and the fitting results. The square points and the solid line denote the experimental data and the fitting results, respectively.

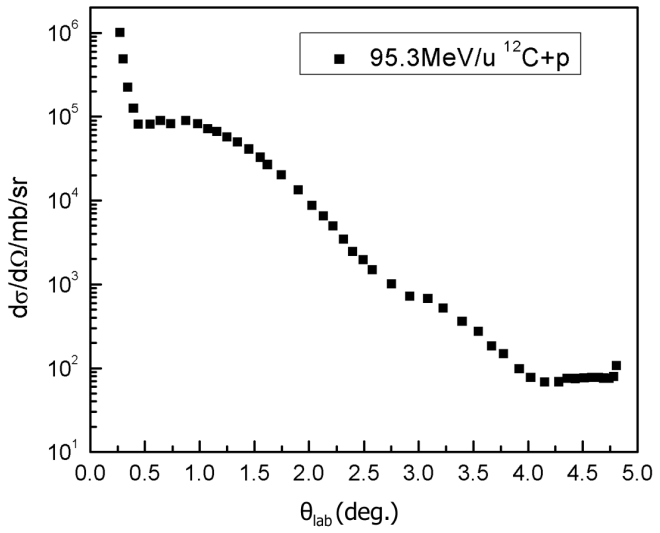

Fig. 4. The angular distribution of $95.3A$ MeV ^{12}C+p elastic scattering in laboratory system.

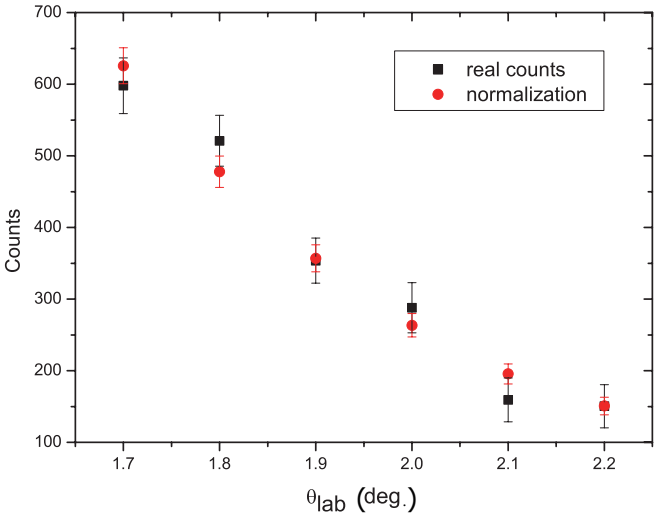

Fig. 5. (Color online) The comparison between the normalized counts (circle) and real counts (square).

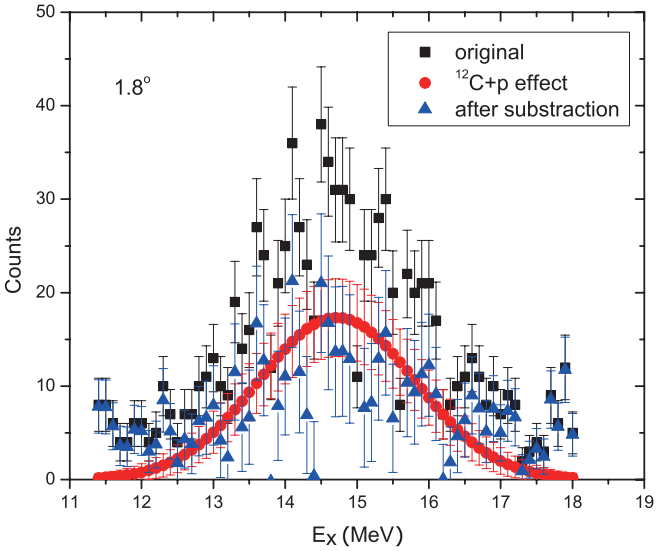

Fig. 6. (Color online) The test of the subtraction of hydrogen disturbance at 1.8°. The original data (square), the effect of $^{12}\mathrm{C}+\mathrm{p}$ elastic scattering (circle) and the result after subtraction (triangle).

Fig. 4. In order to obtain the relationship between the angles and the differential cross sections, the experimental data were fitted from 0.8° to 2.2°. Then we used the fitting function to calculate the differential cross sections from 1.7° to 2.2°, and obtained the ratios between the differential cross sections and the real counts at each angle. The least square method was used to optimize all the ratios. As a result, an optimized ratio, the normalization factor, was given. We then checked the reliability of the normalization factor through the comparison between the normalized counts and real counts, as shown in Fig. 5. It is obvious that all of values are in the range of error bars. So the obtained normalization factor is reasonable. We also checked the results of the uncrossed region of 1.7°–2.2° after the subtraction of the background by using this normalization factor. Fig. 6 shows the result at 1.8°. It is shown that the peak can be subtracted within statistical fluctuation. After that, only the background is left. Therefore, this method for the subtraction of the hydrogen disturbance is reasonable.

We applied this method for the crossed region of 0.9°–1.6°. The above normalization factor is used to calculate the real counts at the crossed regions of 0.9°–1.6°, along with the data from $^{12}\mathrm{C}+\mathrm{p}$ elastic scattering. These deduced counts are acted as the Gaussian distribution in the excitation energy spectra of the $^{12}\mathrm{C}+^{12}\mathrm{C}$ system. The values of the center and the width of the fitted Gaussian distribution in Fig. 3 were transformed to those of $^{12}\mathrm{C}+^{12}\mathrm{C}$ system by using Eq. (6). So the values of the width and the center of the Gaussian dis-

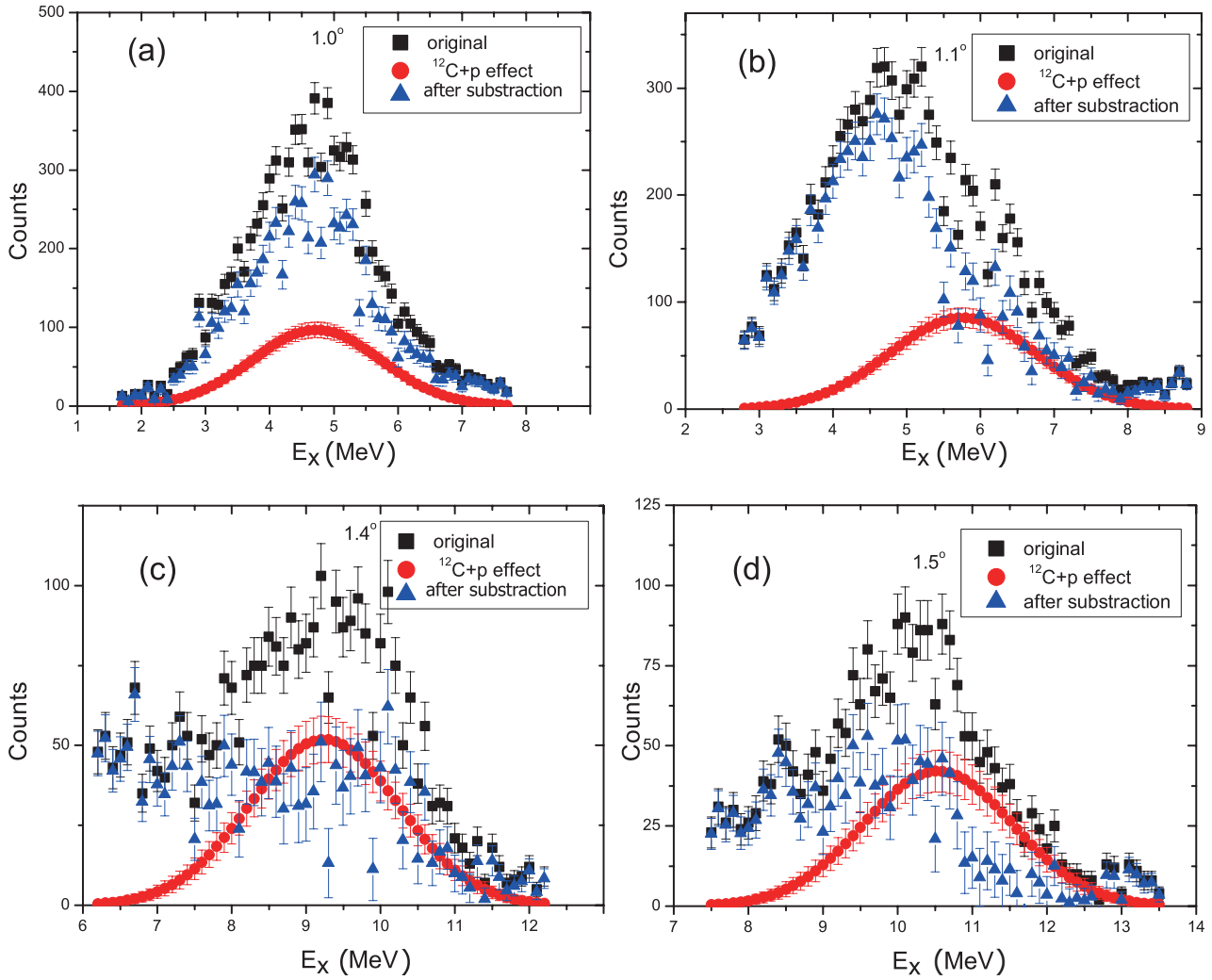

Fig. 7. (Color online) The results of hydrogen subtraction at 1.0°, 1.1°, 1.4° and 1.5°.

tribution in the $^{12}\mathrm{C}+^{12}\mathrm{C}$ system are determined. The width is usually set as 3σ. The results of four examples are shown in Fig. 7. It's obvious that the $^{12}\mathrm{C}+\mathrm{p}$ elastic scattering contribution is large in comparison with that of $^{12}\mathrm{C}+^{12}\mathrm{C}$ in Fig. 7(c).

B. Extraction of hydrogen content in the natural carbon target

The differential cross section is defined as

$$\frac{\mathrm{d}\sigma}{\mathrm{d}\Omega}=\frac{N/\varepsilon_d\varepsilon_t}{N_0N_T\mathrm{d}\Omega}, \tag{7}$$

where N, ε_d, ε_t, N_0, N_T, and $\mathrm{d}\Omega$ denote the counts of reaction events, the detectors efficiencies, the trigger efficiency, the beam intensity, the target number per square centimeter, and the solid angle, respectively. Since we obtained the reacted counts from $^{12}\mathrm{C}+\mathrm{p}$ elastic scattering in the uncrossed region of the fitting in Fig. 3 and the differential cross sections are given from Fig. 4, ε_d, ε_t, N_0, and $\mathrm{d}\Omega$ can be determined according to the experimental arrangement and measurement. Then we can obtain the hydrogen content for each angle. The results are listed in Table 1. Using the weighted

TABLE 1. The results of hydrogen content in the natural carbon target. The first and the second columns represent the angles in the laboratory frame and the real counts of reacted hydrogen deduced from the fitting, respectively. The third column shows the amount of hydrogen per area of the natural carbon target. The relative error of hydrogen content is indicated in fourth column

Angles (deg.)	Real counts	H numbers ($\times10^{18}$/cm^2)	Relative errors (%)
1.7	598	1.58325	6.33
1.8	521	1.81728	6.94
1.9	354	1.64291	8.75
2.0	288	1.81152	12.18
2.1	159	1.34735	20.99
2.2	150	1.65899	20.76

mean method, the final hydrogen content in the natural carbon target is $(2.73 \pm 0.12)\%$.

IV. CONCLUSION

In this paper, we used two-body kinematics to calculate the cross angles of the ground state of $95.3A$ MeV $^{12}\mathrm{C}+\mathrm{p}$ elastic scattering and the excited states of $100A$ MeV $^{12}\mathrm{C}+^{12}\mathrm{C}$, including the 4.4 MeV (2_1^+) state and the 9.64 MeV (3_1^-) state. By using this method, the experimental angles are calibrated and the experimental data are checked. Next, the method and the results of the subtraction of hydrogen contaminant are introduced and discussed, respectively. The elastic scattering of ^{12}C on hydrogen background from the experimental target has a large contribution at some angles, so in the data analysis the contribution of this part needs to be subtracted. Finally, the hydrogen content in the natural carbon target was extracted. The result is $(2.73 \pm 0.12)\%$. At the same time, the method used in present paper can help us improve the future experiment. The experiment using the $(CH_2)_n$ target can calibrate some parameters, such as the efficiencies of the faraday cup, detectors, and so on. It provides a method for nuclear physics experiments.

ACKNOWLEDGMENTS

We thank Prof. Sakaguchi Harutaka from RCNP for his help during the preparation of the experiment. We are also grateful to the RCNP Ring Cyclotron staffs for providing the stable carbon beams throughout the experiment.

[1] Furumoto T and Sakuragi Y. Phys Rev C, 2006, **74**: 034606.
[2] Furumoto T, Sakuragi Y, Yamamoto Y. Phys Rev C, 2008, **78**: 044610.
[3] Furumoto T, Sakuragi Y, Yamamoto Y. Phys Rev C, 2009, **79**: 011601(R).
[4] Furumoto T, Sakuragi Y, Yamamoto Y. Phys Rev C, 2009, **80**: 044614.
[5] Furumoto T, Sakuragi Y, Yamamoto Y. Phys Rev C, 2010, **82**: 044612.
[6] Furumoto T, Horiuchi W, Takashina, *et al*. Phys Rev C, 2012, **85**: 044607.
[7] Furumoto T and Sakuragi Y. Phys Rev C, 2013, **87**: 014618.
[8] Nguyen V, Ye Y, Arvieux J, *et al*. Nucl Phys A , 1987, **464**: 717–739.
[9] Fujiwara M, Akimune H, Daito I, *et al*. Nucl Instrum Meth A, 1999, **422**: 484–488.
[10] Wakasa T, Hatanakaa K, Fujita Y, *et al*. Nucl Instrum Meth A, 2002, **482**: 79–93.
[11] Qu W, Zhang G, Tanihata I, *et al*. Chinese Phys C, 2014, **38**: 116202.
[12] Strauch K and Titus F. Phys Rev, 1953, **103**: 200–208.